

# **Modelling the impact of Temperature-Dependent Specific Heat capacity of $TiO_2$ – $CNTs$ – $SiO_2$ Tri-Hybrid Casson Nanofluid for enhanced Solar Panels**

ASELEBE L. O., OBANSOLA O.Y., TITILADE A.S., OMOLOBA O.

**Federal School of Surveying, Oyo**

**BEING A PAPER PRESENTED AT THE INTERNATIONAL CONFERENCE AND ADVANCED  
WORKSHOP ON MODELLING AND SIMULATION OF COMPLEX SYSTEMS**

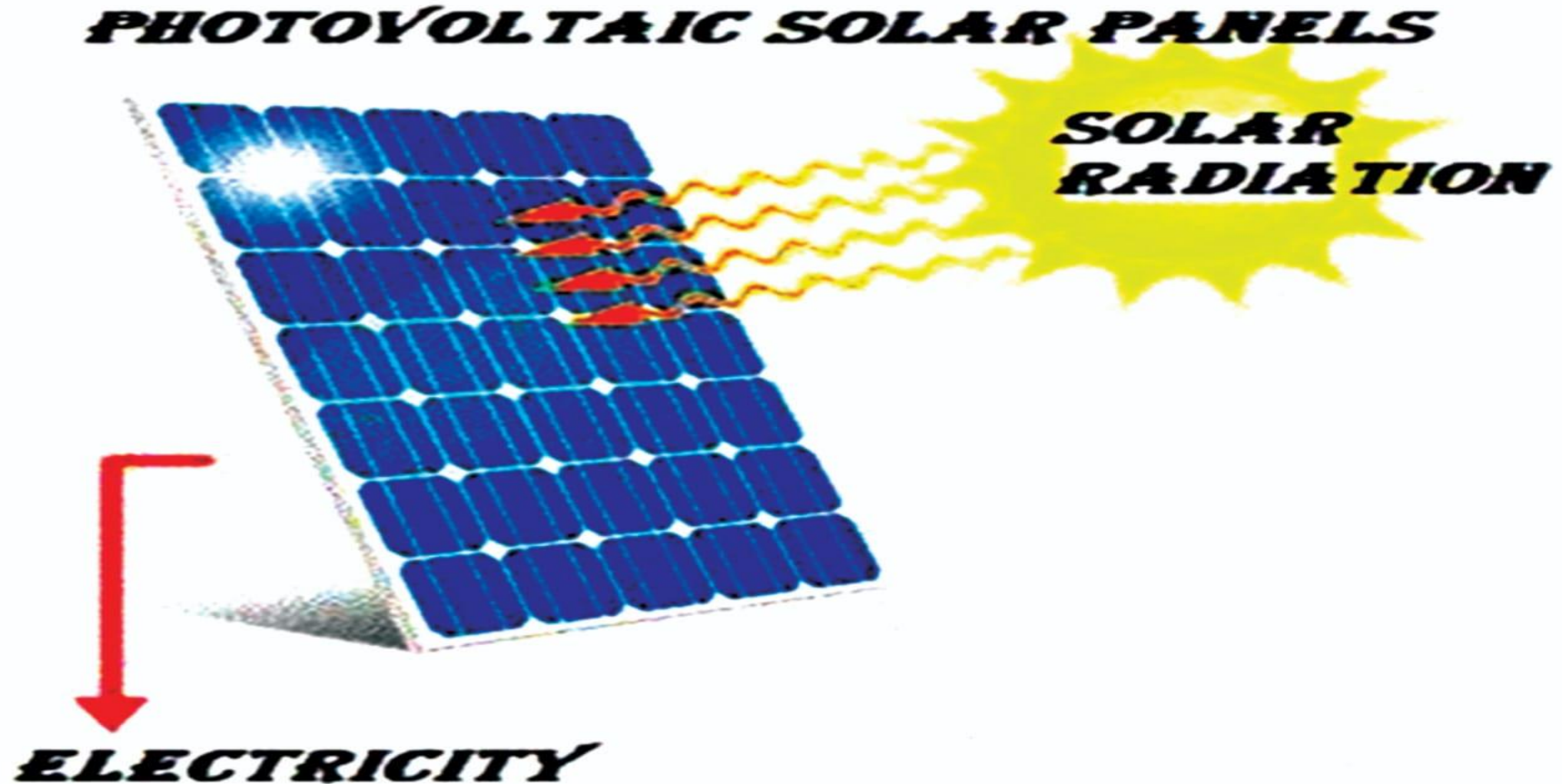
**May 28, 2024.**

# Introduction

- Energy powers our movements, industries, and homes.
- Increasing energy demand due to population growth and economic development leads to reliance on fossil fuels, causing climate change.
- Global warming and rising fuel prices drive the shift towards renewable energy sources like solar, wind, and hydropower.
- Solar energy is crucial for generating electricity and powering various applications with zero greenhouse gases.
- **Challenges:** Weather variability, energy storage issues, and overheating reduce efficiency and battery lifespan.

# Photovoltaic Solar Panels

3



# Nanofluids as a solution to solar panel cooling

4

- Nanofluids enhance thermal conductivity and heat transfer performance.
- Hybrid nanofluids combine multiple nanoparticle types for superior thermal conductivity.
- Tri-hybrid nanofluid achieve remarkable heat transfer properties and are promising for cooling systems in various devices, including solar panels.
- **Challenges:** Nanoparticle stability, agglomeration, and optimizing thermophysical properties

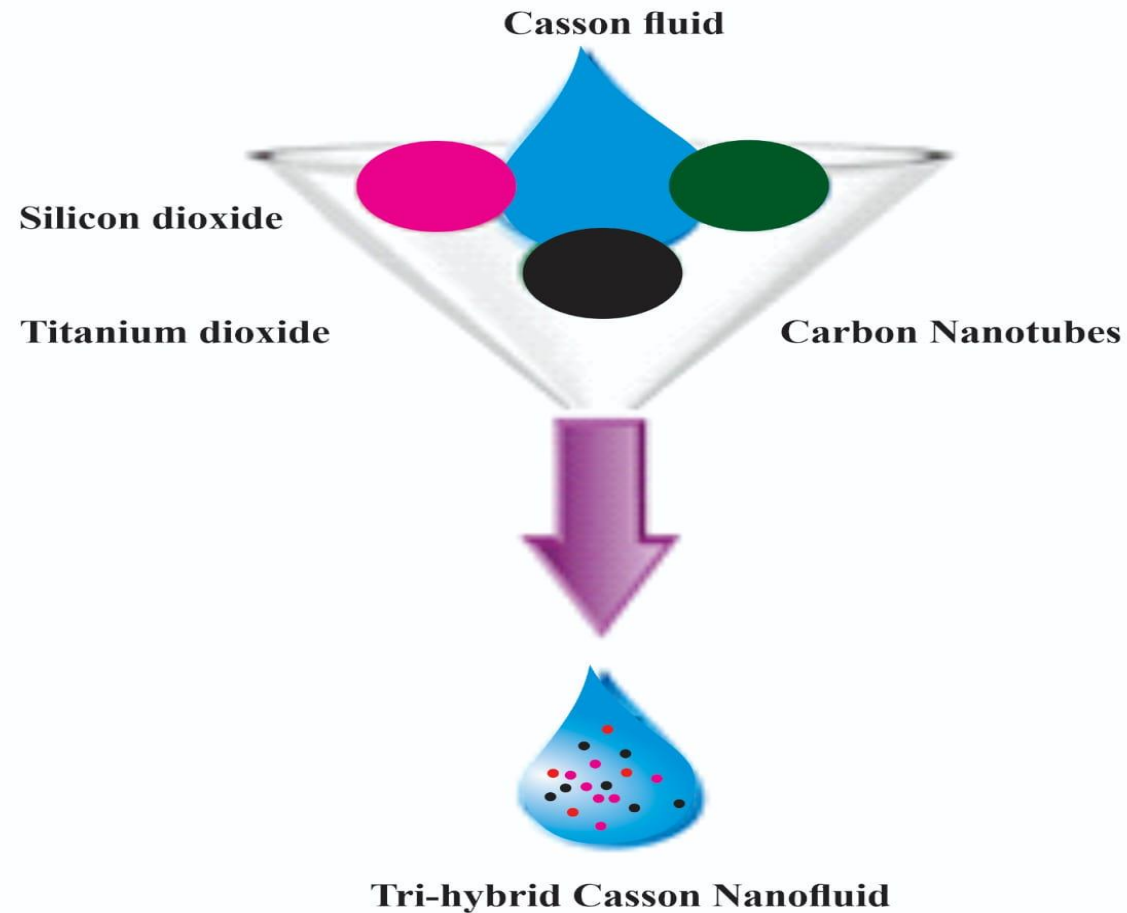
# Tri-Hybrid Casson Nanofluids for Solar Panel Heat Transfer

- 1. Combines Casson Fluid Properties: Shear-thinning behavior improves flow under high shear rates.
- 2. Enhanced Thermal Conductivity: Multiple nanoparticles (e.g., metal oxides, carbon nanotubes) significantly boost heat transfer.
- 3. Improved Efficiency: Better heat absorption and dissipation enhance solar panel performance.
- 4. Optimal Temperature Regulation: Maintains ideal operating temperatures for photovoltaic cells.

# The choice of Nanoparticles

- The three nanoparticles includes Titanium dioxide,  $TiO_2$  , Carbon Nanotubes (CNTs), and Silicon di oxide,  $SiO_2$ .
- The base fluid is **Casson fluid**
- **Why these three Nanoparticles?**
  - $TiO_2$  : enhances thermal conductivity,
  - CNTs : promote efficient photon absorption,
  - $SiO_2$  : aids in emission control.

# What is Tri-Hybrid Casson Nanofluid?



Suspension of Three nanoparticles in Casson fluid

# APPLICATION OF TRI-HYBRID CASSON NANOFUID ON SOLAR PANELS

Tri hybrid  
Casson Nanofluid  
applications  
in solar  
systems

sola cells

solar stills

Terminal Energy  
Storage Systems

Photovoltaic/thermal  
(pv/t) system



# Motivation and Research gap of this study

- **MOTIVATION:**

Researchers aim to improve convective heat transfer rates in solar panels using Tri-Hybrid Casson nanofluids, which are crucial for enhancing photovoltaic efficiency.

- **RESEARCH GAP:**

While previous studies have explored the effects of various properties like thermal conductivity, viscosity, and density of Tri-Hybrid nanofluids on solar panel performance, limited research has been conducted on specific heat capacity, especially considering the variable temperature-dependent aspect.

# AIM AND NOVELTY OF THE WORK

## • **AIM:**

This research aims to bridge this gap by investigating the modeling impact of temperature-dependent specific heat capacity of Tri-Hybrid Casson Nanofluid on solar panel performance.

## • **NOVELTY:**

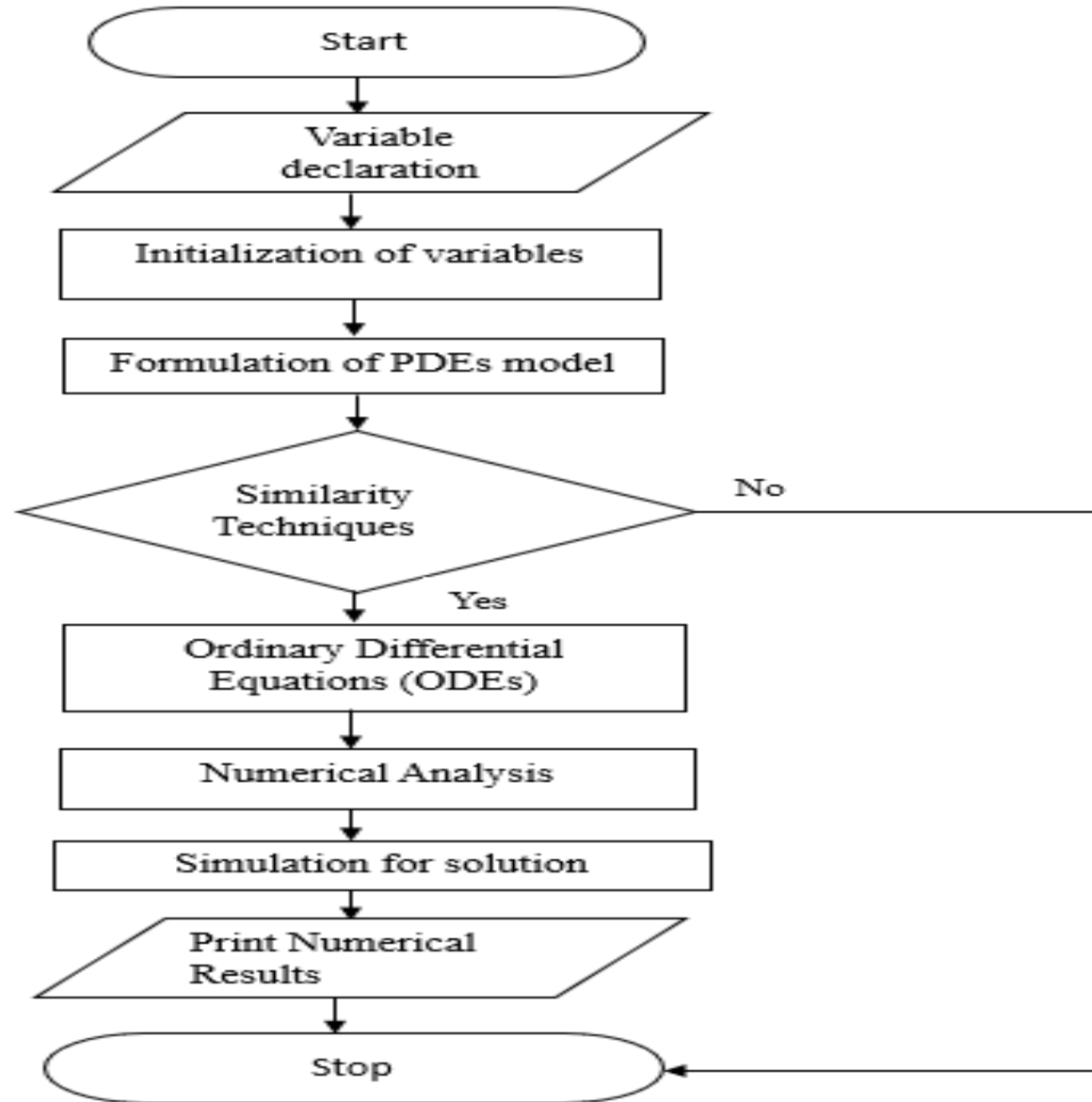
The novelty of this work lies not only in incorporating the variable temperature-dependent specific heat capacity but also in its focus on a unique Tri-hybrid Casson nanofluid formulation with promising properties for solar panel applications.

# OBJECTIVES

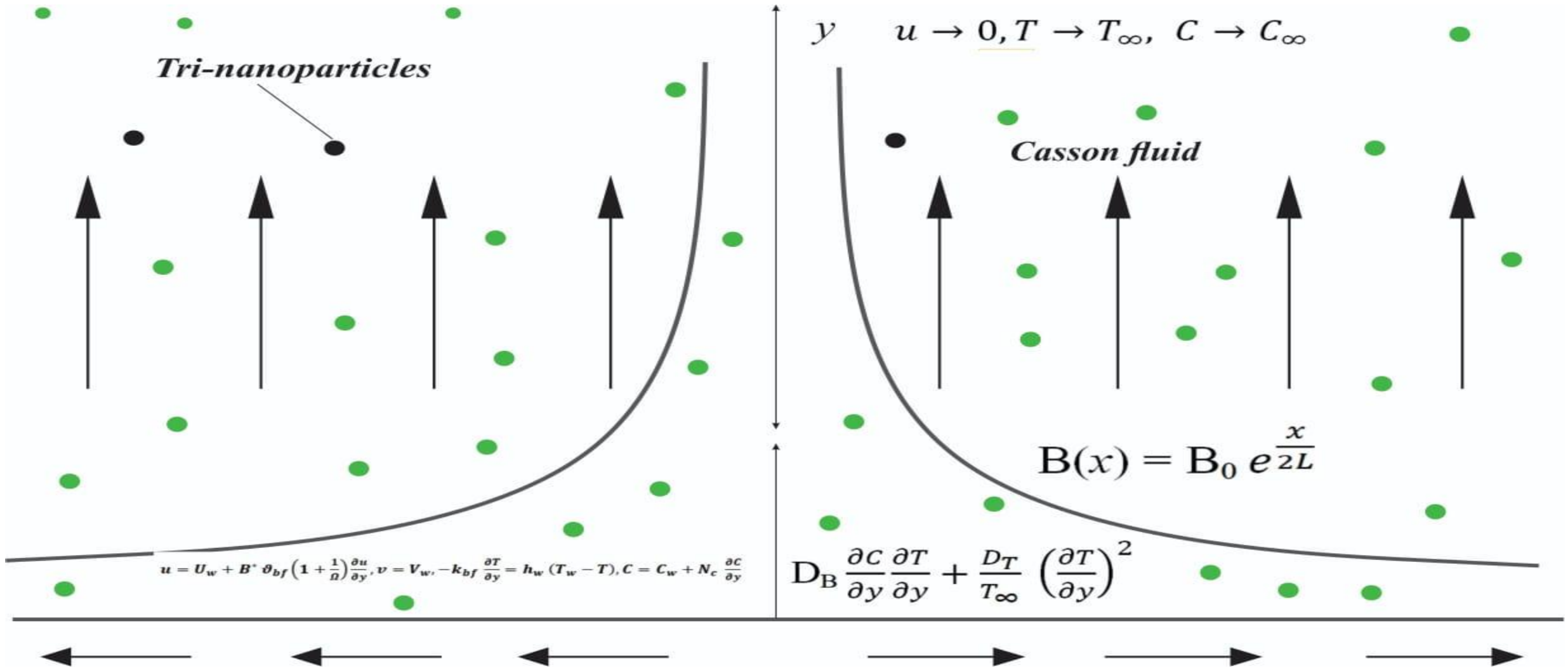
## THE SPECIFIC OBJECTIVES OF THIS WORK ARE TO:

1. formulate a model of the governing Partial Differential Equations (PDEs) and transform them into a system of Ordinary Differential Equations (ODEs) using similarity techniques.
2. solve the ODEs numerically using the Runge-Kutta method of the 4th order alongside the shooting method with the aid of Maple 18.0 software.
3. investigate the effect of the thermophysical parameters of Tri-Hybrid nanofluid on the skin friction, Nusselt number, and Sherwood number, also, on the velocity, temperature and concentration profile.

# FLOWCHART OF THE STUDY



# Description of the problem



# Assumptions

The flow of electrically conducting 2D Tri-Hybrid Casson Nanofluid on exponentially shrinking/stretching surface.

It is considered by incorporating:

- Variable temperature-dependent specific heat capacity,
- magnetic field, and
- thermal radiation.

# Mathematical modelling of the problem

- $$\frac{\partial u}{\partial x} + \frac{\partial v}{\partial y} = 0 \quad (1)$$

- $$u \frac{\partial u}{\partial x} + v \frac{\partial u}{\partial y} = \frac{\mu_{TriNf}}{\rho_{TriNf}} \left( 1 + \frac{1}{\Omega} \right) \frac{\partial^2 u}{\partial y^2} - \frac{\sigma^* B_0^2 u}{\rho_{TriNf}} \quad (2)$$

- $$u \frac{\partial T}{\partial x} + v \frac{\partial T}{\partial y} = k_{TriNf} \frac{\partial}{\partial y} \left( \frac{1}{(\rho C_p)_{TriNf} (T)} \frac{\partial T}{\partial y} \right) - \frac{1}{(\rho C_p)_{TriNF} (T)} \frac{\partial \bar{q}_r}{\partial y} + \tau_w \left[ D_B \frac{\partial C}{\partial y} \frac{\partial T}{\partial y} + \frac{D_T}{T_\infty} \left( \frac{\partial T}{\partial y} \right)^2 \right] \quad (3)$$

- $$u \frac{\partial C}{\partial x} + v \frac{\partial C}{\partial y} = D_B \frac{\partial^2 C}{\partial y^2} + \frac{D_T}{T_\infty} \frac{\partial^2 T}{\partial y^2} \quad (4)$$

# Boundary conditions

- $u = U_w + B^* v_{bf} \left(1 + \frac{1}{\Omega}\right) \frac{\partial u}{\partial y}, v = V_w, -k_{bf} \frac{\partial T}{\partial y} = h_w (T_w - T), C = C_w + N_c \frac{\partial C}{\partial y}$  at  $y=0$  (5)

- $u \rightarrow 0, T \rightarrow T_\infty, C \rightarrow C_\infty$  as  $y \rightarrow \infty$  (6)

- $\overline{q_r} = -\frac{4\sigma^*}{3k^*} \frac{\partial T^4}{\partial y}$  (7)

- $T^4 \approx 4T_\infty^3 T - 3T_\infty^4$  (8)

- $\frac{\partial \overline{q_r}}{\partial y} = -\frac{16\sigma^* T_\infty^3}{3k^*} \frac{\partial^2 T}{\partial y^2}$  (9)



# Properties of Tri-hybrid nanofluids

- The properties of Tri-hybrid nanofluids are defined by [22,23] as:

$$\left. \begin{aligned}
 \mu_{TriNf} &= \frac{\mu_{bf}}{(1 - \phi_{Np1})^{2.5} (1 - \phi_{Np2})^{2.5} (1 - \phi_{Np3})^{2.5}} \\
 \rho_{TriNf} &= \rho_{bf} \left( (1 - \phi_3) \left\{ (1 - \phi_2) \left[ (1 - \phi_1) + \phi_1 \frac{\rho_{Np1}}{\rho_{bf}} \right] + \phi_2 \frac{\rho_{Np2}}{\rho_{bf}} \right\} + \phi_3 \frac{\rho_{Np3}}{\rho_{bf}} \right) \\
 (\rho C_p)_{TriNf} &= (\rho C_p)_{bf} \left( (1 - \phi_3) \left\{ (1 - \phi_2) \left[ (1 - \phi_1) + \phi_1 \frac{(\rho C_p)_{Np1}}{(\rho C_p)_{bf}} \right] + \phi_2 \frac{(\rho C_p)_{Np2}}{(\rho C_p)_{bf}} \right\} + \phi_3 \frac{(\rho C_p)_{Np3}}{(\rho C_p)_{bf}} \right) \\
 \frac{K_{TriNF}}{K_{hNF}} &= \frac{(k_{Np3} + 2k_{hNFF}) - 2\phi_{Np3}(k_{hNF} - k_{Np3})}{(k_{Np3} + 2k_{hNF}) + \phi_{Np3}(k_{hNF} - k_{Np3})}
 \end{aligned} \right\} \quad (10)$$

- The temperature dependent specific heat capacity of Tri-hybrid nanofluid is given as:

$$\bullet \quad (\rho C_p)_{TriNf}(T) = (\rho C_p)_{bf}(T) \left( (1 - \phi_3) \left\{ (1 - \phi_2) \left[ (1 - \phi_1) + \phi_1 \frac{(\rho C_p)_{Np1}}{(\rho C_p)_{bf}} \right] + \phi_2 \frac{(\rho C_p)_{Np2}}{(\rho C_p)_{bf}} \right\} + \phi_3 \frac{(\rho C_p)_{Np3}}{(\rho C_p)_{bf}} \right) \quad (11)$$

# Temperature-dependent Specific heat capacity

18

- where the variable temperature dependent specific heat capacity of base fluid can be given as:

- $$(\rho C_p)_{bf}(T) = (\rho C_p)_{bf} [1 + c(T - T_\infty)] \quad (12)$$

- $$(\rho C_p)_{bf}(T) = (\rho C_p)_{bf} [1 + c(T_w - T_\infty)\theta(\eta)] \quad (13)$$

- $$(\rho C_p)_{bf}(T) = (\rho C_p)_{bf} [1 + \delta\theta(\eta)] \quad (14)$$

- where;

$$\delta = c(T_w - T_\infty)$$

- is the variable temperature-dependent specific heat capacity parameter

# Similarity Techniques

The similarity solution of equations (1) –(6) is achieved by defining the independent variable  $\eta$ , a stream function  $\psi$ , in terms of dependent variables

$f(\eta)$  ,  $\theta(\eta)$  , and  $g(\eta)$  as:

$$\left. \begin{aligned} \psi &= \sqrt{2\nu_{bf} L b e^{\frac{x}{2L}}} f(\eta), \eta = y \sqrt{\frac{b}{2\nu_{bf} L}} e^{\frac{x}{2L}}, \theta(\eta) = \frac{T - T_{\infty}}{T_w - T_{\infty}}, g(\eta) = \frac{C - C_{\infty}}{C_w - C_{\infty}} \\ u &= \frac{\partial \psi}{\partial y} = b e^{\frac{x}{L}} f'(\eta), v = -\frac{\partial \psi}{\partial x} = -\sqrt{\frac{\nu_{bf} b}{2L}} e^{\frac{x}{2L}} f(\eta) - \frac{by}{2L} e^{\frac{x}{L}} f'(\eta) \end{aligned} \right\} \quad (15)$$

Equation (1) is satisfied automatically

# Coupled Nonlinear Ordinary Differential Equations

$$\frac{\Delta_1}{\Delta_2} \left( 1 + \frac{1}{\Omega} \right) f'''' + ff''(\eta) - 2(f')^2 - \frac{Ha}{\Delta_2} f'(\eta) = 0 \quad (16)$$

$$\frac{\Delta_4}{\Delta_3 \text{Pr}} \left( \frac{\theta''}{(1 + \delta\theta)} - \frac{\delta(\theta')^2}{(1 + \delta\theta)^2} \right) + \frac{\theta''}{\text{Pr}(1 + \delta\theta)\Delta_3} Ra + f\theta' + N_B\phi'\theta' + N_T(\theta')^2 = 0 \quad (17)$$

$$\phi'' + Scf\phi' + \frac{N_T}{N_B} \theta'' = 0 \quad (18)$$

# The initial/boundary conditions

$$f(0) = S_u, f'(0) = \alpha + \lambda \left( 1 + \frac{1}{\Omega} \right) f''(0), \theta'(0) = -Bi[1 - \theta(0)],$$

at  $\eta = 0$  (19)

$$\phi(0) = 1 + \Psi g'(0)$$

$$f'(\eta) \rightarrow 0, \theta(\eta) \rightarrow 0, \phi(\eta) \rightarrow 0 \quad (20)$$

# The values of the unknowns

The resulted thermophysical parameters

$$\Delta_1 = \frac{1}{(1-\varphi_1)^{2.5} (1-\varphi_2)^{2.5} (1-\varphi_3)^{2.5}}, \Delta_2 = (1-\varphi_3) \left\{ (1-\varphi_2) \left[ (1-\varphi_1) + \varphi_1 \frac{\rho_{Np1}}{\rho_{bf}} \right] + \varphi_2 \frac{\rho_{Np2}}{\rho_{bf}} \right\} + \varphi_3 \frac{\rho_{Np3}}{\rho_{bf}}$$

$$\Delta_3 = (1-\varphi_3) \left\{ (1-\varphi_2) \left[ (1-\varphi_1) + \varphi_1 \frac{(\rho C_p)_{Np1}}{(\rho C_p)_{bf}} \right] + \varphi_2 \frac{(\rho C_p)_{Np2}}{(\rho C_p)_{bf}} \right\} + \varphi_3 \frac{(\rho C_p)_{Np3}}{(\rho C_p)_{bf}}$$

$$\Delta_4 = \left( \frac{(k_{Np1} + 2k_{bf}) - 2\varphi_1(k_{bf} - k_{Np1})}{(k_{Np1} + 2k_{bf}) + \varphi_1(k_{bf} - k_{Np1})} \right) \left( \frac{(k_{Np2} + 2k_{NF}) - 2\varphi_2(k_{hNF} - k_{Np2})}{(k_{Np2} + 2k_{NF}) + \varphi_2(k_{NF} - k_{Np2})} \right) \left( \frac{(k_{Np3} + 2k_{hNFF}) - 2\varphi_3(k_{hNF} - k_{Np3})}{(k_{Np3} + 2k_{hNF}) + \varphi_3(k_{hNF} - k_{Np3})} \right)$$

# The skin friction, Nusselt number, and Sherwood number

23

The skin friction, Nusselt number, and Sherwood number are the physical quantities of interest and are given as:

$$\begin{aligned} C_{fx} &= \frac{\mu_{TriNf} \left( 1 + \frac{1}{\Omega} \right)}{\rho_{bf} b^2 e^{\frac{3x}{2L}}} \frac{\partial u}{\partial y} \Big|_{y=0} \\ \bullet \quad Nu &= \frac{-k_{TriNf} L}{k_{bf} (T_w - T_\infty) e^{\frac{x}{2L}}} \frac{\partial T}{\partial y} \Big|_{y=0} \\ \bullet \quad S_h &= \frac{-L}{(C_w - C_\infty) e^{\frac{x}{2L}}} \frac{\partial C}{\partial y} \Big|_{y=0} \end{aligned} \tag{21}$$

- After differentiation equation (21) becomes:

$$C_{fx} \sqrt{2 \text{Re}_x} = \frac{1}{(1 - \varphi_1)^{2.5} (1 - \varphi_2)^{2.5} (1 - \varphi_3)^{2.5}} \left( 1 + \frac{1}{\Omega} \right) f''(0)$$

- $$Nu \sqrt{\frac{2}{\text{Re}_x}} = -\frac{k_{TriNf}}{k_{bf}} \theta'(0) \tag{22}$$

$$S_h \sqrt{\frac{2}{\text{Re}_x}} = -g'(0)$$



# Numerical analysis

25

- **Importance of Numerical Methods:**

  - Essential for scientific and engineering disciplines

  - Analytical solutions often elusive for complex Boundary Values Problems

- **Challenges with Boundary Values Problems:**

  - Traditional analytical techniques often inadequate

- **Common Numerical Methods:**

  - Fourth-order Runge-Kutta method
  - Runge-Kutta Fehlberg 45 (RK45) method
  - Adams-Bashforth method
  - Finite difference method
  - Finite element method

# Shooting Method

- **Shooting Method:**

- Robust approach for coupled nonlinear BVPs
- Converts BVPs to initial value problems (IVPs)
- Iteratively refines guessed initial conditions
- Ensures solution meets boundary constraints

# Numerical method cont'd

The above coupled nonlinear third-order ordinary differential equations are reduced into a system of first order ordinary differential equations (ODEs) by letting:

$$\begin{aligned} f = n_1, f' = n_1' = n_2, f'' = n_2' = n_3, f''' = n_3' = n_4, \theta = n_5, \theta' = n_5' = n_6, \theta'' = n_6' = n_7, g = n_8 \\ g' = n_8' = n_9, g'' = n_9' = n_{10} \end{aligned} \quad (23)$$

Substituting the equation (23) into equations (16)-(20) give the required system of first order ODEs as:

$$\bullet \quad f''' = n_3' = n_4 = \frac{2\Delta_2}{\Delta_1\left(1 + \frac{1}{\Omega}\right)} (n_2)^2 + \frac{Ha}{\Delta_1\left(1 + \frac{1}{\Omega}\right)} n_2 - \frac{\Delta_2}{\Delta_1\left(1 + \frac{1}{\Omega}\right)} n_1 n_3 \quad (24)$$

$$\begin{aligned} \theta'' = n_6' = n_7 = & \frac{\Delta_4 \delta}{(\Delta_4 + Ra)(1 + \delta n_5)} (n_6)^2 - \frac{\Delta_3 (1 + \delta n_5)}{(\Delta_4 + Ra)} \text{Pr} n_1 n_6 \\ \bullet \quad & - \frac{\Delta_3 (1 + \delta n_5)}{(\Delta_4 + Ra)} \text{Pr} N_B n_9 n_6 - \frac{\Delta_3 (1 + \delta n_5)}{(\Delta_4 + Ra)} \text{Pr} N_T (n_6)^2 \end{aligned} \quad (25)$$

$$\phi'' = n_9' = n_{10} = -Sc n_1 n_9 - \frac{N_T}{N_B} n_7 \quad (26)$$

# Numerical method cont'd

$$n_1(0) = S_u, n_2(0) = \alpha + \lambda \left(1 + \frac{1}{\Omega}\right) a, n_3(0) = a, n_5(0) = b, n_6(0) = -Bi[1 - b],$$
$$n_8(0) = 1 + \Psi c, n_9(0) = c$$

The shooting method is used to guess the unknowns  $a, b$ , and  $c$  until the boundary conditions  $n_2(\infty), n_5(\infty)$ , and  $n_8(\infty)$  are satisfied. The resulting differential equations are solved numerically using the 4<sup>th</sup> order Runge-Kutta method.

# Results and Discussions

Table 1: The Thermophysical properties of Casson fluid, and nanoparticles, ( $TiO_2$ ,  $SiO_2$  and CNTs) [37].

Thermophysical Properties	Casson fluid $C_6H_9NaO_7$	$TiO_2$	$SiO_2$	CNTs
Thermal conductivity, (W/mk)	0.6376	8.9568	36	6600
Specific Heat Capacity, ( $J.kg^{-1}k^{-1}$ )	4175	686.2	765	425
Density, ( $Kg/m^3$ )	989	4250	3970	2600

# Results of Numerical method

31

In order to validate the correctness of this study the values of  $f''(0)$ ,  $-\theta'(0)$ , and  $-g'(0)$  were compared with the work of [1] and excellent agreement was established.

**Table 2: Comparison with [1] for  $Pr = 6.2, Ra = \delta = Sc = S_u = 0, \Omega = \infty$ ,  $N_B = 0.1$**

$N_T$	Work of [1] $f''(0)$	Present work $f''(0)$	Work of [1] $-\theta'(0)$	Present work $-\theta'(0)$	Work of [1] $-g'(0)$	Present work $-g'(0)$
<b>0.1</b>	-1.28180857	-1.28124179	0.25373483	0.25317044	0.37525393	0.37535393
<b>0.2</b>	-1.28180857	-1.28124179	0.25191726	0.25194002	0.20422841	0.29314672
<b>0.3</b>	-1.28180857	-1.28124179	0.25007701	0.25000529	0.03660735	0.03761834
<b>0.4</b>	-1.28180857	-1.28124179	0.24821431	0.24822423	-0.1275704	-0.12762371
<b>0.5</b>	-1.28180857	-1.28124179	0.24632921	0.24632848	-0.2882678	-0.28923355

# Result and discussion

Table 3: Impact of Variable Specific heat capacity,  $\delta$  , on  $f''(0)$ ,  $-\theta'(0)$ , and  $-g'(0)$

$\delta$	$f''(0)$	$-\theta'(0)$	$-g'(0)$
0.05	- 0.146139249388517	1.52528741156937	- 0.580452428264102
0.1	- 0.146139249388215	1.56372271766941	- 0.614171468055997
0.5	- 0.146139249387869	1.83449564070648	- 0.852057072534243
1.0	- 0.146139249387676	2.10666386278441	- 1.09166714124498
Slope	<b>7.84369E-13</b>	<b>0.612852162</b>	<b>-0.538890398</b>



# Result and discussion

Table 4: Effect of Thermal Radiation,  $Ra$  on  $f''(0)$  ,  $-\theta'(0)$  , and  $-g'(0)$

$Ra$	$f''(0)$	$-\theta'(0)$	$-g'(0)$
0.5	- 0.146139249392372	1.25782516007649	- 0.348803216534943
1.0	- 0.146139249399646	1.06827684439477	- 0.185589731477336
3.0	- 0.146139249462864	0.703477537747997	0.128807741903066
5.0	- 0.146139249456675	0.547066217410380	0.268165579581688
<b>Slope</b>	<b>-1.59883E-11</b>	<b>-0.153819157</b>	<b>0.133488189</b>

# Result and discussion

Table 5: Effect of Casson parameter,  $\Omega$ , on  $f''(0)$ ,  $-\theta'(0)$  and  $-g'(0)$

$\Omega$	$f''(0)$	$-\theta'(0)$	$-g'(0)$
0.5	- 0.146139249388517	1.52528741156937	- 0.580452428264102
1.0	-0.199721438431961	1.53685311826791	- 0.597481889444215
3.0	- 0.273925515780488	1.54822224925624	-0.623153963390784
5.0	- 0.297521408058996	1.55105959357199	-0.631090133375942
<b>Slope</b>	<b>-0.0318084</b>	<b>0.005208544</b>	<b>-0.010734733</b>

# Effect of variation of thermophysical parameters on temperature profile

35

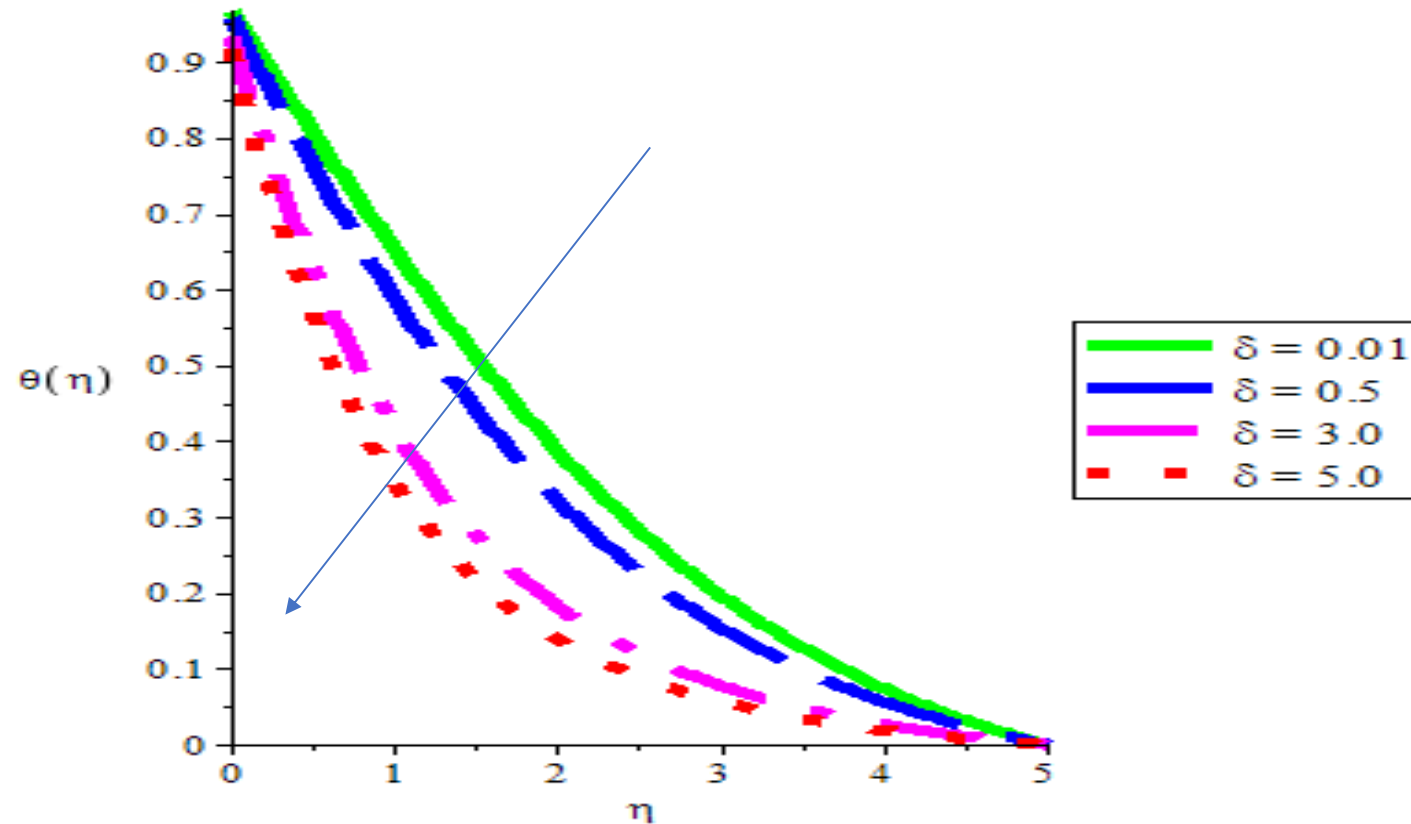


Figure 2: Temperature profile varying  $\delta$

# Effect of variation of thermophysical parameters on temperature profile

36

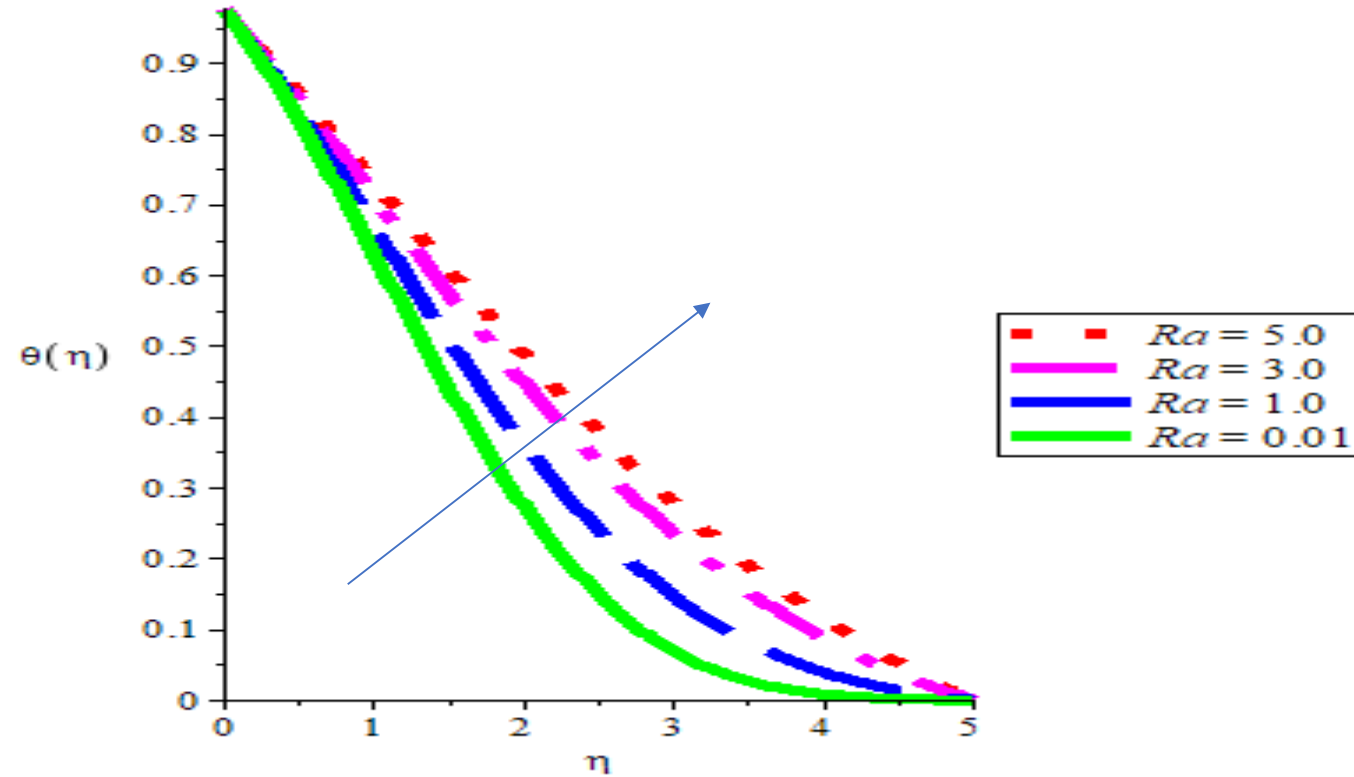


Figure 3: Temperature profile varying  $Ra$

# Effect of variation of thermophysical parameters on temperature profile

37

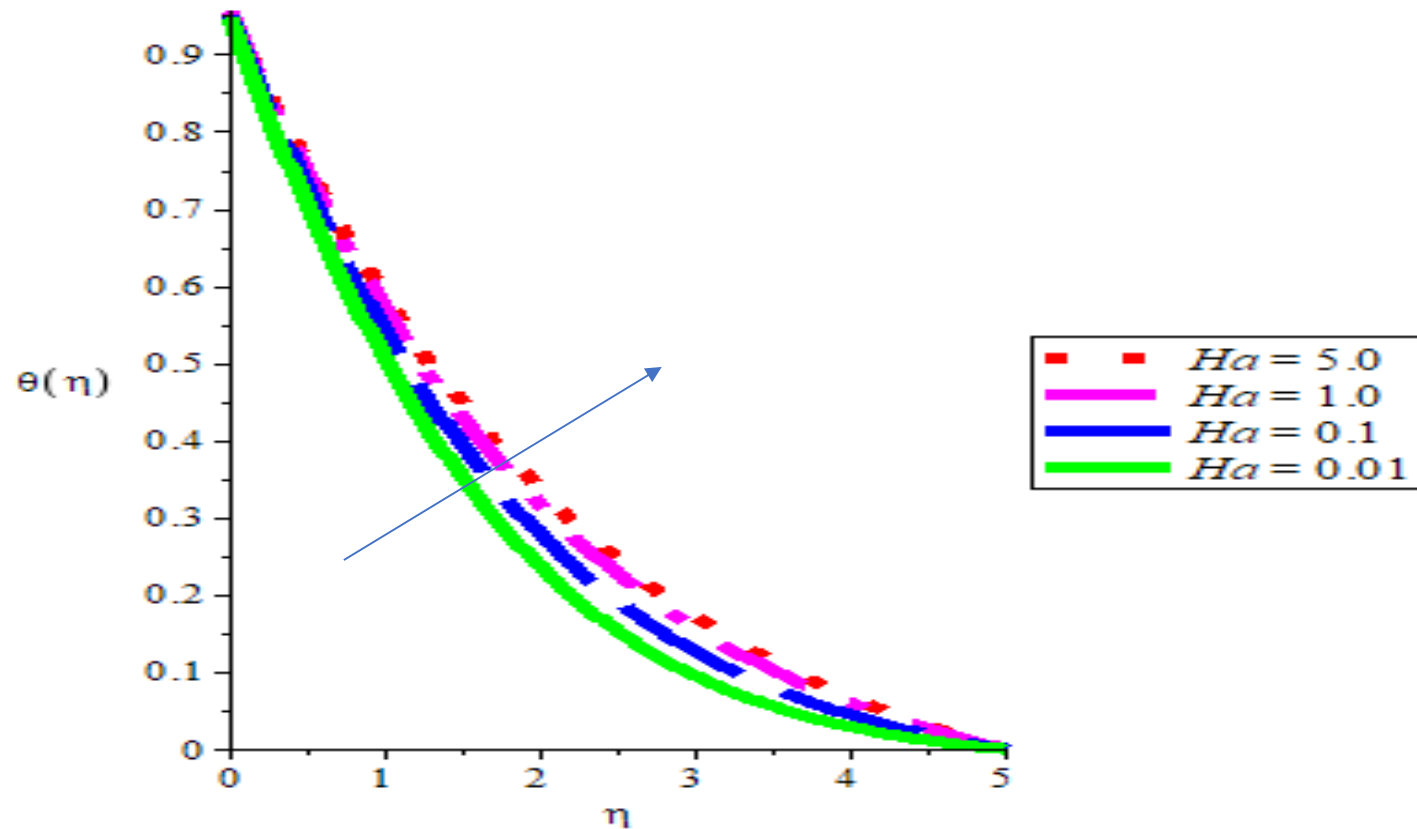


Figure 4: Temperature profile varying  $Ha$

# Effect of variation of thermophysical parameters on velocity profile

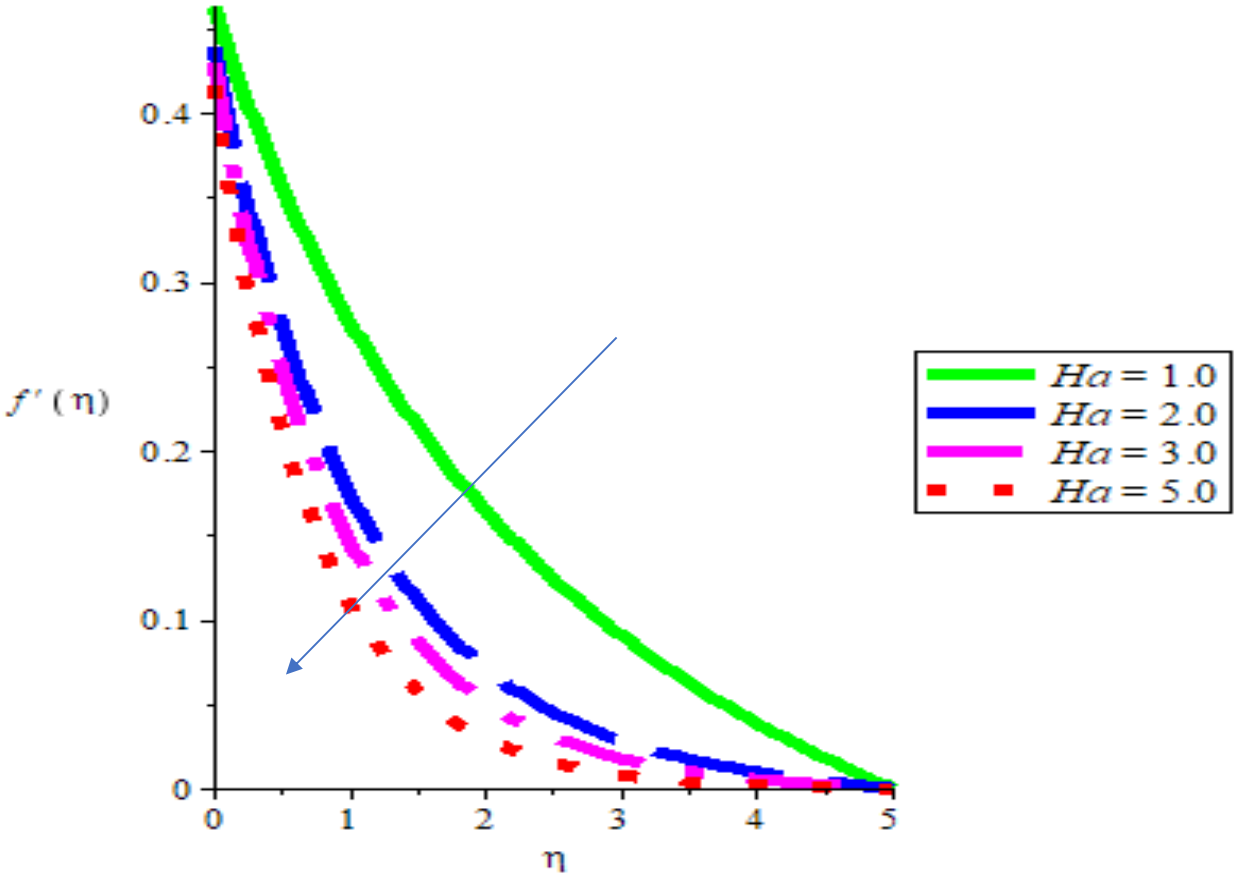


Figure 5: Velocity profile varying  $Ha$

# Effect of variation of thermophysical parameters on velocity profile

39

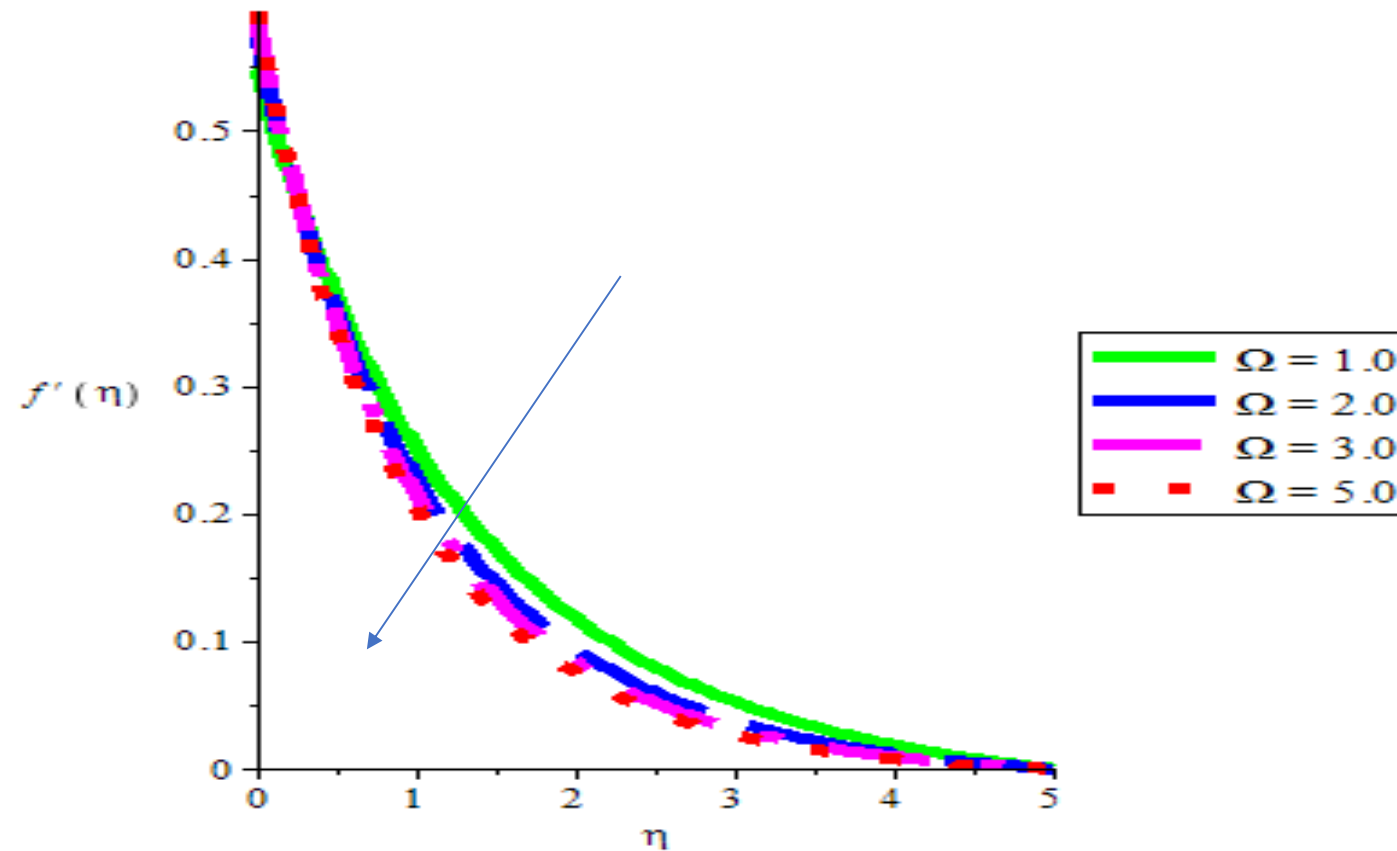


Figure 6: Velocity profile varying  $\Omega$

# Effect of variation of thermophysical parameters on Concentration profile

40

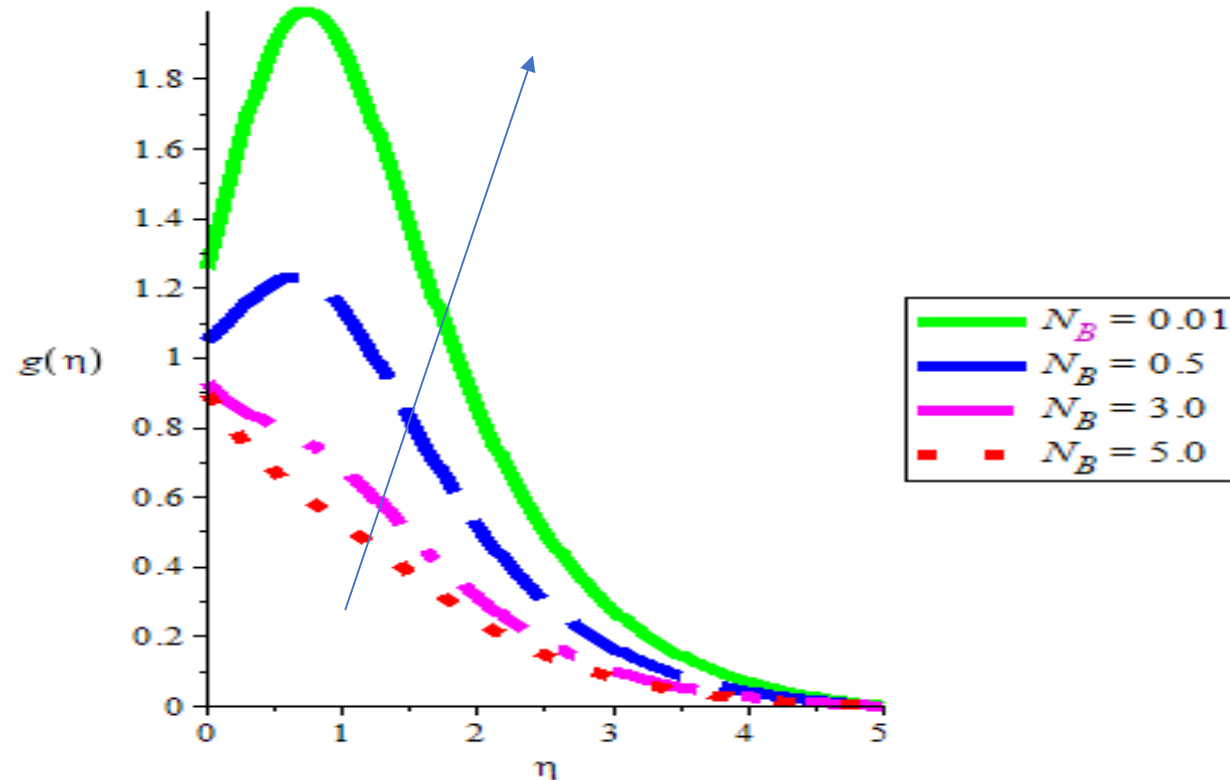


Figure 7: Concentration profile varying  $N_B$



# Effect of variation of thermophysical parameters on Concentration profile

41

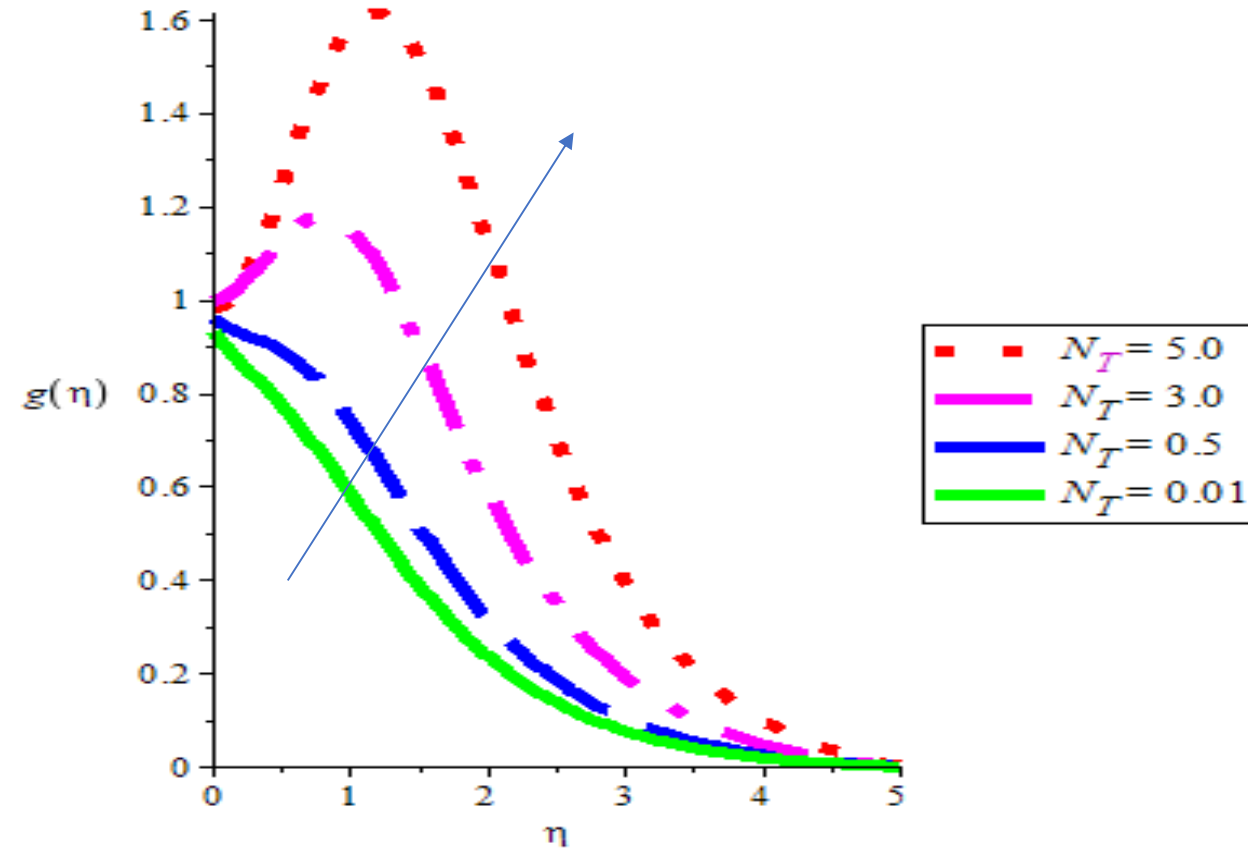


Figure 8: Concentration profile varying  $N_T$

# Conclusion

- Explored Tri-hybrid Casson nanofluids for improved solar panel cooling.
- Integrated temperature-dependent specific heat capacity into thermal modeling.
- Found significant potential for optimizing heat transfer and enhancing efficiency.
- Insights support the development of more effective and sustainable solar panels.

# Future work

- Experimental validation and diverse nanoparticle analysis recommended.
- This research paves the way for advanced solar energy systems with extended lifespan and reliability.

# References

- [1] Lund LA, Omar Z, Khan I, M.Sherif E, Abdo HS. Stability Analysis of the Magnetized Casson Nanofluid Propagating through an exponentially Shrinking/Stretching plate: Dual Solutions. *Symmetry*, 2020, 12, 1162, doi:10.3390/sym12071162.
- [2] Alhassan CJ, Achema KO, Ogor MO. Exploring Numerical Methods for Solving Boundary Value Problem: A study of Finite Difference and Shooting Methods with MATLAB Implementation. *Global Scientific Journals*. 2023; 11, 8, [www.globalscientificjournal.com](http://www.globalscientificjournal.com).
- [3] Ida N. Boundary Value Problems: Numerical (Approximate) Methods. In: Engineering Electromagnetics. *Springer, Cham*.2021; 285-333. [https://doi.org/10.1007/978-3-030-15557-5\\_6](https://doi.org/10.1007/978-3-030-15557-5_6)

# References

- [4] Ajala OA, Aselebe LO, Abimbade SF, Ogunsola AW. Effect of magnetic fields on the boundary layer flow of heat transfer with variable viscosity in the presence of thermal radiation. *International Journal of Scientific and Research Publications*, 9 (5) (2019) 2250-3153. DOI: 10.293322/IJSRP.9.05.2019. p8904.
- [5] Rathore N, Sandeep N. Solar thermal energy performance on mono/tri-hybrid nanofluid flow through the evacuated thermal collector tube. *International Journal of Hydrogen Energy*. 2023; 48(94):36883-36899. Rathore N, Sandeep N. Solar thermal energy performance on mono/tri-hybrid nanofluid flow through the evacuated thermal collector tube. *International Journal of Hydrogen Energy*. 2023 Dec 5;48(94):36883-99. <https://doi.org/10.1016/j.ijhydene.2023.06.029>
- [6] Rtimi, B., Benhmidene, A., Hidouri, K., Chaouachi, B. (2023). Use of Nanofluid to Improve the Efficiency of Photovoltaic Panel. In: Khiari, R., Jawaid, M. (eds) *Proceedings of the 3rd International Congress of Applied Chemistry & Environment (ICACE–3)*. ICACE 2022. Springer Proceedings in Materials, vol 23. Springer, Singapore. [https://doi.org/10.1007/978-981-99-1968-0\\_4](https://doi.org/10.1007/978-981-99-1968-0_4)

*Thanks for your  
attention!!!*